1995MNRAS.276..923R

Mon. Not. R. Astron. Soc. **276,** 923–932 (1995)

A study of the Orion cometary cloud L1616

B. Ramesh★

Raman Research Institute, C. V. Raman Avenue, Sadashivanagar, Bangalore 560080, India

Accepted 1995 April 27. Received 1995 April 27; in original form 1994 November 25

ABSTRACT

With its cometary appearance and a reflection nebula near its edge facing some bright Orion stars, Lynds' cloud L1616 shows ample evidence of being affected by one or more of these massive stars. To estimate its mass and star formation efficiency, as well as to determine if it is gravitationally bound, we mapped this cloud in $J = 1 \rightarrow 0$ transitions of ^{12}CO and ^{13}CO. It is found that the distribution of the emission in the line *wings* shows clear evidence for substantial mass motions. Also, the 'virial' mass of the cloud is found to be five times the actual cloud mass determined from the ^{13}CO column density map. It is argued that this cloud has abnormally high star formation efficiency and is possibly disintegrating. The morphology and the location of the cloud indicate that it is being affected by the star ε Orionis, which is also (possibly) responsible for the cloud's unusual star formation efficiency. Over a range of values of the relevant parameters, the star is found to satisfy quantitatively the requirements of being the cause of the observed characteristics of the cloud.

Key words: stars: formation – ISM: clouds – ISM: individual: L1616 – reflection nebulae – radio lines: ISM.

1 INTRODUCTION

Massive stars substantially affect the structure and the evolution of the clouds around them. Globules and clouds with bright rims and cometary appearance are found in the vicinity of many nearby OB associations e.g. Vela (Gum nebula; Sridharan 1992), Orion (Bally et al. 1991), Cepheus (Indrani & Sridharan 1994) and Rosette (Patel, Xie & Goldsmith 1993). In addition to affecting the morphology, these stars also accelerate the globules and possibly induce star formation. There are many clouds in the Orion complex which show evidence of being affected by nearby stars. Lynds' dark cloud L1616 with its cometary appearance is one among them. It also harbours a bright reflection nebula NGC 1788, also known as CED 040, excited by a poor star cluster.

Study of a cloud with an associated reflection nebula offers many advantages. Since reflection nebulae mark close spatial association of relatively dense interstellar clouds with luminous stars of spectral type B1 or later, the distance to the star and hence to the cloud can be estimated to a reasonable accuracy. This allows one to determine sizes, masses and luminosities reliably. A reflection nebula with newly-born stars provides an opportunity to study the effects of recent formation of stars with intermediate masses. In particular, one that harbours a new-born cluster is most suited to study cloud fragmentation. Stars, newly-formed or otherwise, have significant effects on the thermal balance of a cloud. Hence, study of such a cloud where there is an identifiable dominant energy source (but not as disruptive as O stars) permits one to investigate the heating and cooling in them.

L1616 appears to be unique among the reflection nebulae. As shown in the next section L1616 has an estimated star formation efficiency of ~ 14 per cent, much larger than other clouds with associated reflection nebulae. The cometary appearance of the cloud, the peculiar location of the nebula near its edge facing the bright Orion-belt stars, and its suspected high star formation efficiency indicate that the cluster formation in the cloud has possibly been induced. Furthermore, no *IRAS* source with a spectrum typical of young stellar objects is found within the cloud boundary. This may suggest that the formation of the cluster has pre-empted any further star formation – a self-regulatory process often invoked in the literature. Thus, L1616 seems to be an object of considerable interest. We mapped this cloud in $J = 1 \rightarrow 0$ transitions of both ^{12}CO and ^{13}CO with a view to determining its mass more reliably and to discern any mass motions that may be present. In this paper, we present the maps and argue that induced star formation is most likely to be the case and also that the cloud is fragmentating.

In the following section, we estimate the star formation efficiencies (SFEs) of a few clouds with associated reflection

★ E-mail: bram@rri.ernet.in

© Royal Astronomical Society • Provided by the NASA Astrophysics Data System

1995MNRAS.276..923R

nebulae, and show that L1616 is unique among them. In Section 3 we present the details of the observations and the maps of L1616. The results are discussed in Section 4.

2 SFE OF CLOUDS WITH REFLECTION NEBULAE

Star formation efficiency (SFE) usually refers to the ratio of the total mass of the stars to the sum of this stellar mass and the mass of the cloud or cloud segment in which they are born. We estimate the masses in these two components for the bright reflection nebulae in the following way using optical and infrared data from the literature.

Masses of the clouds. The cloud mass can be expressed as $2 \times N(H_2)\, m(H) \Omega_C d^2$, where $N(H_2)$ is the molecular hydrogen column density, $m(H)$ the atomic mass of hydrogen, Ω_C the solid angle of the cloud and d its distance from the Sun. To estimate Ω_C and $N(H_2)$ reliably, the clouds need to be mapped in both ^{12}CO and ^{13}CO. However, for most of the reflection nebulae such maps are not available. Hence, we use their optical obscuration solid angles listed in the catalogues of dark clouds (Lynds 1962; Feitzinger & Stuwe 1984; Hartley et al. 1986). We wish to note that only the mass in dense portions of the cloud, which the optical obscuration would trace well, may be relevant for the estimation of SFE. The molecular hydrogen column density seems to be nearly constant in clouds over a wide range of sizes (Larson 1981) and we take this to be $\sim 5 \times 10^{21}$ cm^{-2}, typical of the small molecular clouds. The masses estimated in this way will be very approximate. Nevertheless, we believe that this will not be a severe handicap for the relative comparison of SFE attempted here.

Masses in stars. Many optically bright reflection nebulae are also bright in the far-infrared (FIR) and have been detected by *IRAS*. Their FIR emission results from reprocessing of the radiation from the exciting stars by the dust in the surrounding cloud. In most cases, the spectral type of the brightest member of the exciting stars is also known. Then, if one assumes all stars to be of the same spectral type, a lower limit to the mass of the stars is given by $4\pi d^2\, S_{FIR} M (\eta L)^{-1}$. Here M and L, respectively, are the mass and luminosity of the brightest star in the cluster derived from its spectral type (Allen 1976), η is the fraction of the stellar radiation that is reprocessed, which is taken to be 0.3 (albedo = 0.7, Witt & Schild 1986) and S_{FIR} is the FIR flux density derived in the following way using the measured flux densities in the four *IRAS* bands (Margulis, Lada & Young 1989):

$$S_{FIR} = \int S_\nu \, d\nu$$
$$= 2.37 \times 10^{-10} \left(S_{12} + 0.567 S_{25} + 0.154 S_{60} + 0.059 S_{100} + \frac{7.39 S_{\lambda_{max}}}{\lambda_{max}} \right) \text{erg s}^{-1}\,\text{cm}^{-2}. \quad (1)$$

In this expression, the flux densities are in Jy; λ_{max}, the longest wavelength at which the flux density is measured, is in μm; and $S_{\lambda_{max}}$ is the corresponding flux density. The last term is the estimated flux emitted longward of λ_{max} (Myers et al. 1987). This is obtained by assuming that $S_{\lambda_{max}}$ is also the maximum over the entire spectrum, and that the spectrum is like that of a blackbody for wavelengths longer than λ_{max}. However, it should be noted that if star formation is *very* recent, as the luminosities of protostars change considerably with time (Lada 1991), the above estimate of mass in stars can be inaccurate.

Since the masses of both the components depend similarly on the distance their ratio is independent of it, resulting in the following expression for the minimum SFE.

$$SFE\,(\text{per cent}) = 100 \left(\frac{X}{1+X} \right)$$

where,

$$X = \frac{M_*}{M_C} = \left(\frac{4\pi S_{FIR} M}{\eta L} \right) \times \frac{1}{(2 m_H N_{H_2} \Omega_C)} = 1.286 \times 10^9 \frac{(M/M_\odot)}{(L/L_\odot)} \frac{(S_{FIR}/\text{erg s}^{-1}\,\text{cm}^{-2})}{(\Omega_C/\mu\ \text{steradian})}. \quad (2)$$

Thus, the only quantities entering the estimates are: the solid angle of the clouds, the *IRAS* flux densities of the associated nebulae and the mass and the luminosity of the exciting star with the earliest spectral type. We use this approach to determine the SFE of a few of the clouds that have associated reflection nebulae. In Table 1 we have listed the names of the nebulae (row 1), of the brightest stars exciting them (row 2), their spectral type (row 3), mass (row 4) and luminosity (row 5), the names of the associated clouds (row 6), their solid angle (row 7) and mass (row 8), names of the associated extended *IRAS* sources (row 9), their flux densities in the four bands (rows 10–13), the FIR fluxes S_{FIR} (row 14), and their estimated SFE (row 15). The spectral type of the stars exciting the nebulae have been taken from the catalogues of reflection nebulae (van den Bergh 1966; van den Bergh & Herbst 1975). Table 1 shows that L1616 has the highest estimated SFE. Two other clouds, L1630 and SC064, also have a high estimated SFE but their masses are likely to be underestimates owing to their large physical sizes. This can be seen from the following. One could take the volume density of molecular hydrogen, n_{H_2}, in the clouds to be the same instead of the column density. Then, for spherical clouds, the new SFE_V is given by

$$SFE_V\,(\text{per cent}) = 100 \left(\frac{X_V}{1+X_V} \right)$$

where,

$$X_V = 1470 \times \frac{X}{(d/\text{pc})(\sqrt{\Omega_C/\mu\ \text{steradian}})}. \quad (3)$$

A value of 1100 cm^{-3} has been assumed for n_{H_2} such that the SFE and SFE_V are the same for the cloud L1616 (this choice does not affect the relative values of SFE_V derived). Row 16 in Table 1 lists SFE_V calculated this way using distances (last row) taken from the literature (Racine 1968; Herbst 1975).

© Royal Astronomical Society • Provided by the NASA Astrophysics Data System

1995MNRAS.276..923R

Table 1. Reflection nebulae – star formation efficiencies.

Nebula	vdB017	vdB013	vdB033	vdB052	vdB055	vdB123	VHE05	VHE30	VHE17	VHE28
Star	+30°549	+30°540	293815	37903	38023	170634				
SpT	B8V	B8V	B9V	B1.5V	B4V	B7V	*	*	B1V	B5Vp
M_* ($M_\odot$)	4.1	4.1	3.6	12.7	7.7	4.7	3.2	3.2	14.2	6.5
L_* ($L_\odot$)	179	179	117	6887	1406	283	79	79	9727	794
Cloud	L1450	L1452	L1616	L1630	L1641	L572	SC025	SC102	SG033	SC064
Ω_C (μstr.)	358	358	12	611	611	1322	171	764	8	212
M_C ($M_\odot$)	6739	2227	157	13862	6617	18935	22279	52259	547	3991
IRAS	X0326	X0322	X0504	X0539	X0539	X1827	X0809	X0916	X0833	X0857
name	+312	+307	−034	−019	−081	+012	−356	−482	−405	−435
12μm (Jy)	91	6	30	2090	52	32	3	14	117	984
25μm (Jy)	30	6	68	177700	53	65	4	28	190	4410
60μm (Jy)	1080	20	323	93400	304	375	14.5	196	1100	26400
100μm (Jy)	1190	49	594	77400	787	750	29	392	2700	24300
S_{FIR} (10^{-10})	1024	45	467	302246	553	536	27	266	1784	25530
SFE (%)	0.84	0.04	13.42	10.55	0.06	0.09	0.08	0.18	4.04	11.32
SFE_V (%)	0.13	0.01	13.42	1.23	0.01	0.01	0.01	0.01	2.20	2.47
Dist. (pc)	501	288	417	550	380	437	1318	955	955	501

A (*) mark in SpT row indicates that the earliest stellar spectral type is not known and has been assumed to be A0V. In cloud name prefix L stands for Lynds' cloud, SC for southern dark cloud and SG for southern dark globule.

Table 1 shows that SFE_Vs for the two clouds, L1630 and SC064, are much smaller than that of L1616. Nevertheless, they also appear peculiar and merit further studies. Before leaving this section, we wish to emphasize that the SFEs calculated here are very approximate. When the estimated stellar mass is a minimum the calculated SFE is a lower limit. This is made quite uncertain, however, because of the error in the estimate of the cloud mass. For example, the assumption that the density is the same for all the clouds may not be valid. In this sense, that both of the small clouds (L1616 and SG033) have high SFEs may be a bias effect resulting from them being denser. Thus, detailed CO observations are needed to confirm these SFEs. We have carried out such observations for the cloud L1616.

3 OBSERVATIONS

The above estimates suggest that, among the clouds with associated reflection nebulae, the cloud L1616 has an abnormally high SFE. However, as mentioned already, it is necessary to make detailed CO maps to determine the cloud mass and hence the SFE more reliably. Such maps would also help to ascertain if mass motions are present. For this purpose, we mapped the cloud L1616 in $J = 1 \rightarrow 0$ transitions of ^{12}CO and ^{13}CO with a ~1 arcmin beam and a grid-point spacing of one beamwidth. The observations were carried out during the 1990–91 and 1991–92 winters using the 10.4-m millimeterwave telescope at the Raman Research Institute campus, Bangalore (for a brief description of the telescope see Patel 1990; Sridharan 1993). A filter-bank spectrometer with 250-kHz (0.65 km s^{-1}) resolution covering a total bandwidth of 64 MHz was used. During the observations, pointing was checked by beam-switched continuum scans on Jupiter (see Patel 1990 for details) and the rms pointing error was estimated to be ~12 arcsec. An ambient temperature load was used for calibration. During the observations the double side band (DSB) T_{sys} ranged from 600 to 1200 K. Frequency switching of 15.25 MHz was used for all the observations and the spectra obtained were appropriately combined. Third-order polynomials were fitted to estimate and remove the curved baselines. Most of the final spectra had an rms noise of ~0.25 K and the estimated rms error on the velocities is ~0.3 km s^{-1}. We estimate the forward spillover and scattering efficiency, η_{fss}, to be 0.57 and 0.63 at the ^{12}CO and ^{13}CO frequencies, respectively, by comparing the measured antenna temperatures on the calibration sources (mostly Ori A) with the source brightness temperatures reported in the literature (taken to be 73 and 16 K at the two frequencies, respectively, for Ori A). We have also corrected the spectra for the elevation dependence of η_{fss}.

The kinetic temperature and the ^{13}CO column density were obtained from the spectra using the relations given by Dickman (1978), assuming that ^{13}CO is optically thin, and that both ^{12}CO and ^{13}CO have the same excitation temperatures. These relations take into account the 2.7-K microwave background, as well as the fact that the usual Rayleigh–Jeans approximation ($= I_{12_{CO}}\, h\nu \ll kT$) is not valid at mm wavelengths for the typical kinetic temperatures that are obtained in the molecular clouds. Figs 1 to 4 show the distributions of the ^{13}CO column density, the kinetic temperature, the equivalent width and the integrated line intensity ($= I_{12_{CO}} \int T\,dV$) in the cloud L1616. The ^{12}C spectra were used to obtain the last three quantities while the ^{13}CO spectra yielded the first. The ellipse in Figs 1 to 4 outlines the *I*-band image of the nebula NGC 1788 (see Plate 62 of Witt & Schild 1986) associated with L1616. Its major and minor axes are ~3.4 and ~2.1 arcmin long, respectively. It is centred at the position of the *IRAS* source with RA = $5^h4^m25^s.8$ and Dec. = −3°25′5″ (hereafter, the *centre*) and oriented 45°

© Royal Astronomical Society • Provided by the NASA Astrophysics Data System

1995MNRAS.276..923R

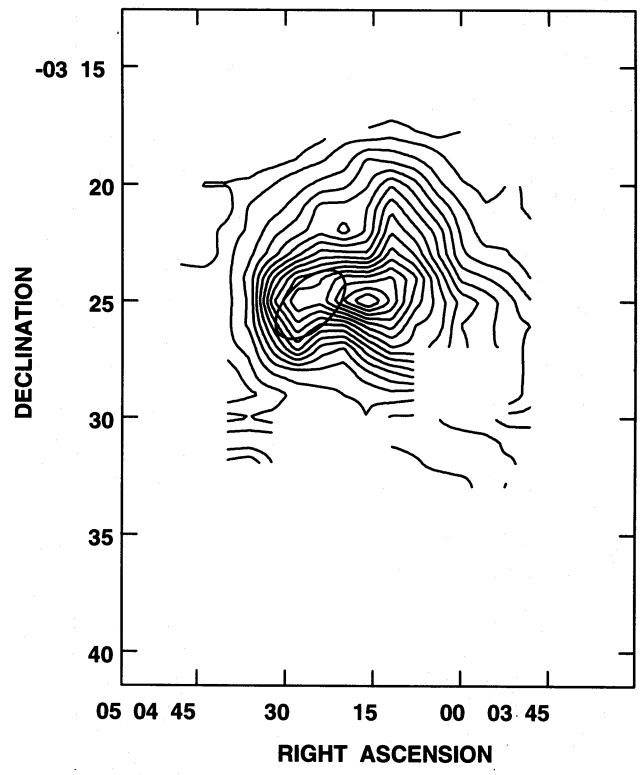

Figure 1. Distribution of ^{13}CO column density in L1616. The ellipse marks the position, the orientation and the extent of the *I*-band image of NGC 1788. The peak contour level is 3.2×10^{16} cm^{-2} and the spacing is 0.2×10^{16} cm^{-2}.

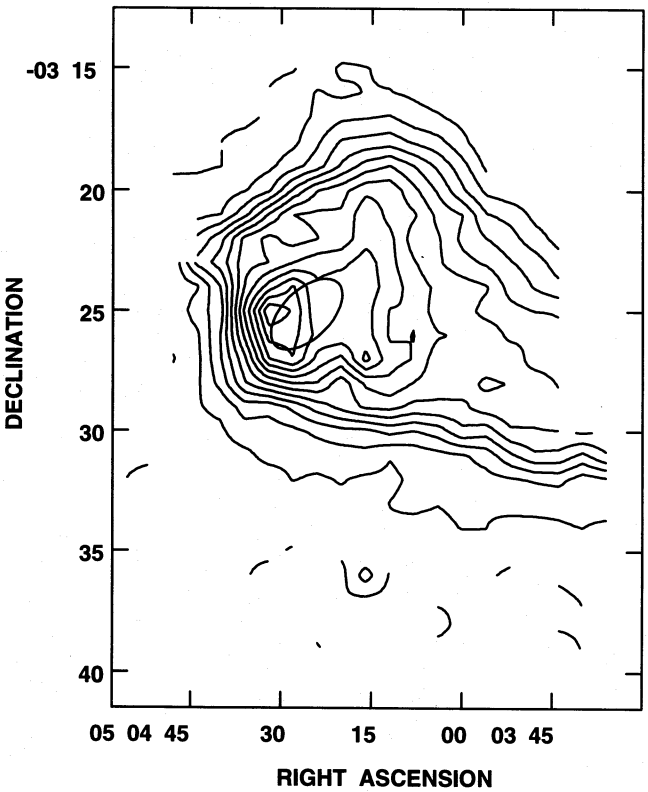

Figure 2. Distribution of ^{12}CO kinetic temperature in L1616. The elliptical outline of the *I*-band image of NGC 1788 is shown. The peak contour level is 30 K and the spacing is 2 K.

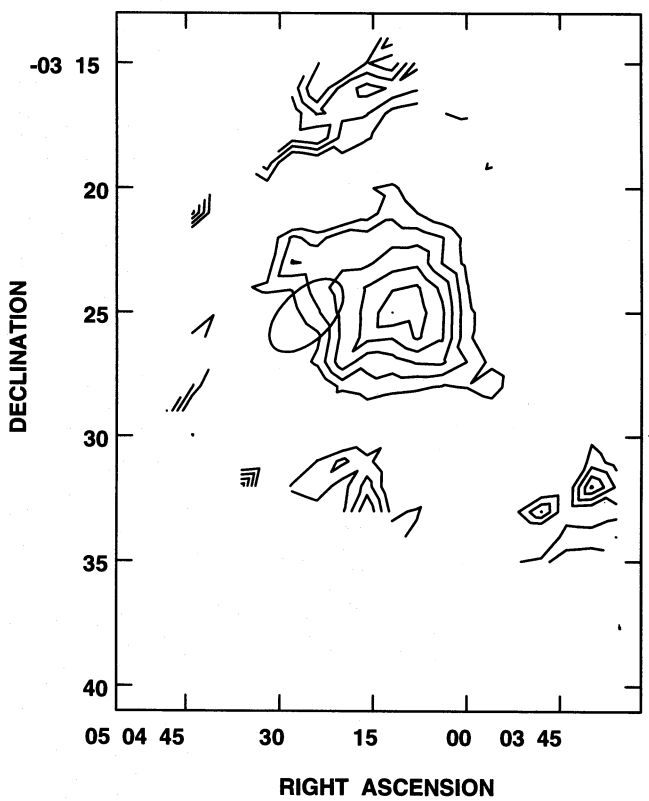

Figure 3. Distribution of equivalent width obtained from ^{12}CO spectra. The innermost contour level is 3.1 km s^{-1} and the spacing is 0.2 km s^{-1}. The outer open contours are possibly artefacts arising from the uncertainty in the measured widths owing to poorer signal-to-noise ratios. The portions of the cloud material lying between the open and closed contours have linewidths $\gtrsim 2$ km s^{-1}, but are not shown for the sake of clarity. The ellipse outlines the *I*-band image of NGC 1788.

with respect to the west. The star, HD 293815, of spectral type B9V is the brightest visible member of the cluster of stars illuminating the nebula NGC 1788. It lies ~0.8 arcmin away from the centre in the north-west direction.

Following are the notable features in the maps.

(1) The ^{13}CO column density peaks at ~3 arcmin west of the centre with a *shoulder* around the nebula, and falls off gradually and more or less symmetrically from the peak.

(2) The temperature distribution is more or less centred on the nebula with its peak at 1 arcmin east of the centre and hence not coincident with the column density peak. This indicates that the radiation from the stars is the dominant energy source.

(3) The spatial distribution of equivalent widths is more or less symmetrically distributed and has its peak coincident with the column density peak. Fig. 3 shows that most parts of the cloud have equivalent linewidths greater than ~2 km s^{-1}.

(4) The contour map of the derived *integrated* ^{12}CO *line intensity* distribution in L1616 bears similarity to both ^{13}CO column density (Fig. 1) and kinetic temperature (Fig. 2) distributions. For example, the two peaks, one each to the east and west of the centre, correspond to the temperature and column density peaks, respectively. This similarity

© Royal Astronomical Society • Provided by the NASA Astrophysics Data System

1995MNRAS.276..923R

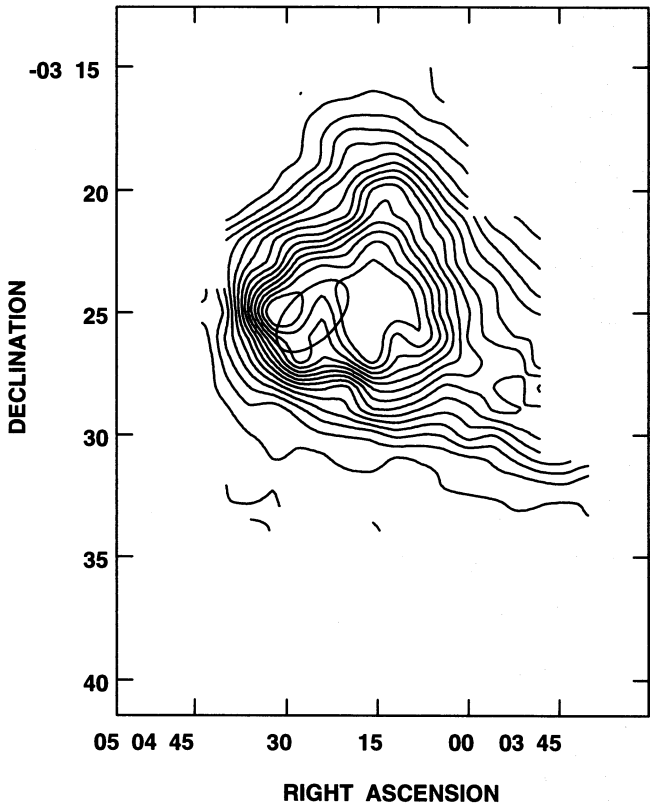

Figure 4. Distribution of integrated ^{12}CO line intensity in L1616. The *I*-band image of NGC 1788 is outlined by the eclipse. The peak contour level is 33 K km s^{-1} and the spacing is 2 K km s^{-1}.

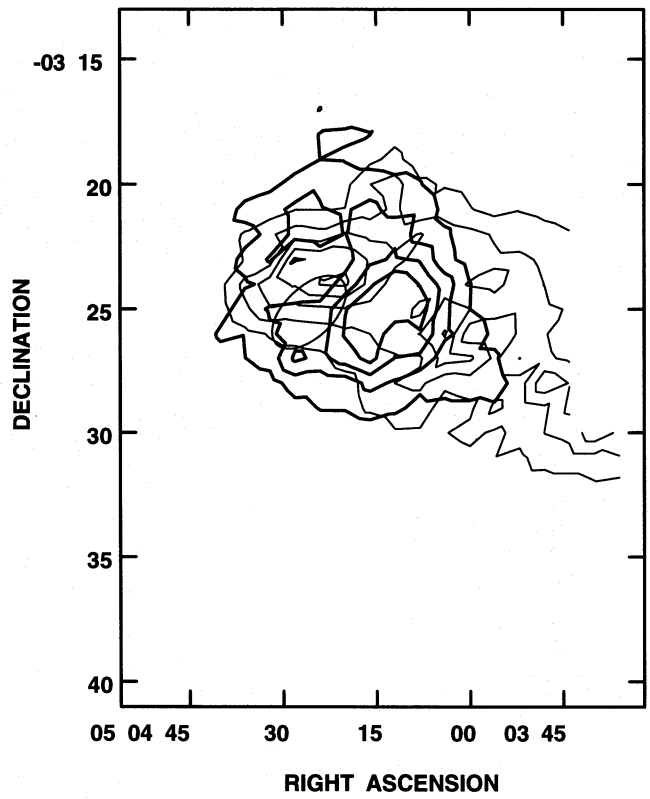

Figure 5. The *thin* and *thick* contours show the distribution of ^{12}CO emission averaged over the velocity ranges 5.4 to 6.7 km s^{-1} and 8.7 to 10.4 km s^{-1}, respectively. The elliptical *I*-band image of NGC 1788 is also marked. The peak contour level is 5 K with a spacing of 1 K.

implies that although the ^{12}CO integrated line intensity map has column density information, it is substantially altered by the distribution of the temperature in the cloud. Hence, using integrated ^{12}CO line intensities to trace the column density distributions of molecular hydrogen is not always reliable.

4 DISCUSSION

As stated earlier, one of the primary objectives of the observations was to determine the cloud mass more reliably. The mass of the cloud estimated from the ^{13}CO column density map presented in the previous section using an N_{H_2} to $N_{13_{CO}}$ conversion factor of 5×10^5 (Dickman 1978) is ~ 169 M$_\odot$. One can also use the integrated ^{12}CO line intensity map to determine the cloud mass. The mass found this way using a value of 2.3×10^{20} cm^{-2} (K km s^{-1})$^{-1}$ for the $I_{12_{CO}}/N_{H_2}$ ratio (Strong et al. 1988) is ~ 193 M$_\odot$. The two mass estimates are in good agreement with each other. We take their mean, which is ~ 180 M$_\odot$, to be the cloud mass. This agrees well with our rough estimate presented in the beginning, although larger by a factor of ~ 1.15. The SFE calculated using this new and more reliably determined cloud mass is ~ 12 per cent (estimated total mass of the stars/stellar and cloud mass). This is still large compared to the average SFE value of $\lesssim 3$ per cent (Evans & Lada 1991) found for the nearby molecular clouds.

One can also obtain the mass from the cloud-averaged linewidth, provided that the cloud is in virial equilibrium. For L1616, since the line is wide over most part of the clouds, the actual cloud-averaged linewidth turns out to be ~ 2.7 km s^{-1}. The corresponding virial mass required to keep the cloud bound is 1000 M$_\odot$, five times larger than the estimated mass. Conversely, if the cloud is bound, its detected mass of ~ 180 M$_\odot$ would imply a cloud-averaged linewidth of only ~ 1.25 km s^{-1}. Thus, it appears that the energy input from the stars in the cluster is *fragmenting* the cloud. The excess turbulent motions of ~ 1.5 km s^{-1} over and above that needed for virial equilibrium and the present cloud size of ~ 2 pc suggest that the fragmentation has possibly been happening for the past 1 to 2 Myr.

The spatial distributions of emission in the *linewings* shown in Fig. 5 also indicate the disturbed state of the cloud. The average emission from the material in the velocity ranges 5.4 to 6.7 km s^{-1} (thin) and 8.7 to 10.4 km s^{-1} (thick), respectively, are shown superimposed one over the other. The blueshifted and redshifted emissions have large spatial extents and distinct peaks, each a little away from the centre. They clearly indicate that substantial mass motion is present, possibly caused by the activity of the stars in the cluster. For example, the spherical redshifted emission, whose peak is coincident with the column density peak, is found to contain ~ 10 per cent of the cloud mass. The conclusion that the mass motions in the cloud is substantial is further supported by the coincidence of the column density peak with the linewidth peak. It is also consistent with the conclusion of de Vries et al. (1984) who, from a systematic survey of reflection nebulae, found that 60 per cent of the clouds with associated

© Royal Astronomical Society • Provided by the NASA Astrophysics Data System

1995MNRAS.276..923R

reflection nebulae have broad lines; the enhanced emission in the wings and local line broadening arise from mass motions resulting from the dynamical interaction between the molecular cloud and the stars illuminating the nebulae. Incidentally, the energy contained in the mass motions is $\sim 10^{45}$ erg, which is less than ~ 0.1 per cent of the energy radiated by the stars in the cluster over the past few million years.

Having found that the cloud L1616 has an abnormally high SFE and shows clear signs of disintegration, we set out to determine the possible cause. Its high SFE and cometary appearance suggest an external cause. Fig. 6 presents a wide-angle view of the portion of the sky around the cloud L1616 showing its cometary tail towards 30° south-west and all nearby stars of spectral type earlier than B2. Only stars such as these can affect the morphology and kinematics of nearby clouds significantly as well as cause implosion in them. Table 2 provides the details of these stars taken from the literature (Hirshfeld & Sinnott 1985). The projected tail is directed nearly perpendicular to the galactic plane and its extension points to stars 3 and 4 as possible causes. However, when their distances from the cloud and their spectral types are considered, it is clear that star 3 (ε Orionis, a blue supergiant) is the most influential one. Its present surface temperature and luminosity estimated from its spectral type (B0Ia) are $\sim 28\,000$ K and 2.5×10^5 $L_\odot$, respectively (Allen 1976). This implies that the spectral type of its main-sequence (MS) progenitor is O6 with a mass of ~ 35 $M_\odot$ and a lifetime of ~ 4.3 Myr. Such a star may have accelerated the cloud through the *rocket effect* (Oort & Spitzer 1955), as well as causing it to implode and form the star cluster. Earlier works (e.g. Bertoldi 1989; Bertoldi & McKee 1990) have shown that a cloud can implode as well as acquire a tail structure in such a process. A simple estimate of the time taken by the cloud to cover the current star–cloud separation of 50–70 pc using the typical induced velocities of 10–15 km s^{-1} (Bertoldi & McKee 1990) yields a value of ~ 5 Myr. That this is in good agreement with the expected age of the star ε Orionis suggests that its progenitor could have propelled the cloud L1616 to its present position from an initial location close to the star within the stellar lifetime. In the following, we proceed to check this suggestion more quantitatively.

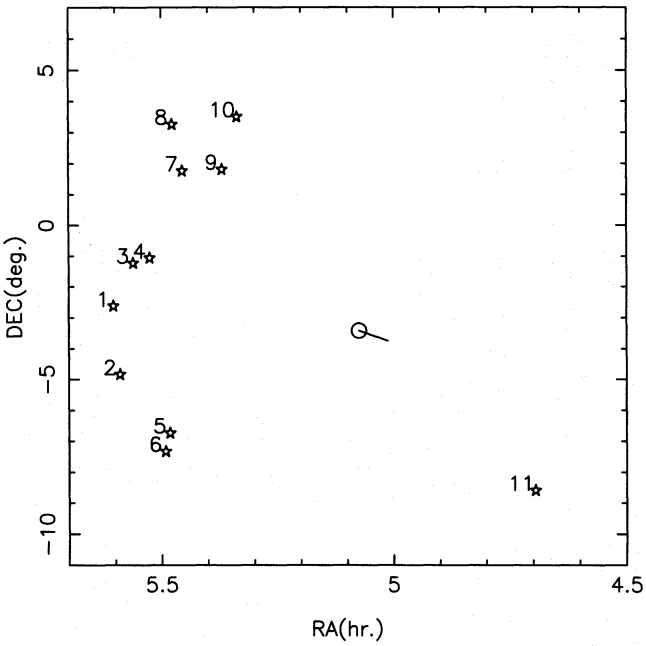

Figure 6. Bright Orion stars near the cloud L1616. Its cometary tail is indicated. The details of the stars are given in Table 2. The tail, when extended points to stars 3 and 4. Star 3 is ε Orionis, a blue supergiant. Owing to its nearness to the cloud and earlier spectral type, the progenitor of ε Orionis is more likely to be responsible for both the morphology and the efficient star formation of the cloud L1616.

Using two dimensionless parameters, viz. the column density parameter, $\log(\eta)$, and the initial shock velocity parameter, $\log(\nu)$, Bertoldi (1989) has classified clouds that are exposed to ionizing radiation. The cloud L1616, given its radius of ~ 1 pc and molecular hydrogen density of 1200 cm^{-3}, has a value of ~ 3.24 for $\log(\eta)$. The upper and lower bounds to its initial distance of 50 pc (set by the present projected cloud separation) and 1 pc, respectively, constrain $\log(\nu)$ to lie between -0.62 and 1.08. These values for the parameters place L1616 in region II of Bertoldi's fig. 1. In this case, almost all of the ionizing radiation will be absorbed by the

Table 2. Luminous stars near the cloud L1616.

Index no.	SAO no.	Dist. pc.	SpT	α_{1950} h m s	δ_{1950} ° ′ ″
1	132406	500	O9.5V	5 36 14	−2 37 39
2	132387	540	B1.5V	5 35 25	−4 50 32
3	132346	370	B0Ia	5 33 41	−1 13 56
4	132269	560	B2V	5 31 31	−1 04 07
5	132210	550	B2V	5 28 55	−6 44 41
6	132222	560	B0V	5 29 31	−7 20 13
7	112830	560	B1.5V	5 27 19	+1 45 05
8	112861	470	B1.5V	5 28 37	+3 15 21
9	112734	490	B1V	5 22 09	+1 48 08
10	112697	470	B1V	5 20 12	+3 29 52
11	131451	460	B2V	4 41 41	−8 35 44
	L1616	420	Cloud	5 04 30	−3 25 00

© Royal Astronomical Society • Provided by the NASA Astrophysics Data System

1995MNRAS.276..923R

recombining gas streaming off the ionization front, and the ionization front can be considered thin relative to the cloud size. In this approximation, the temporal evolution of the parameters (mass, radius, ion density, distance and speed) of a cloud exposed to radiation from a massive star are described by the equations presented in Appendix A. There are three unknowns in the problem: the escape velocity of the ionized plasma, v_i, the fractional cloud velocity at present, v_l/v_i and the ratio of the initial and the final values of the cloud distance, x_0/x_1. The latter two are not independent (as can be seen from equation A4), however, thus reducing the independent unknowns to two. The only constraint is that the cloud moves from x_0 to x_1 within the interaction timescale set by the age of the star. This is bound by its MS lifetime of ~4.3 Myr and its maximum age of ~5 Myr.

Fig. 7 shows a contour plot of the time needed to move to the present separation, taken to be 50 pc, as a function of x_0 and v_i. For the same value of v_i two initial positions, one closer to the star and another closer to the cloud, result in the same time to travel. The former solution is preferred, as it results in a larger average density enhancement ahead of the shock front [which goes as $\ln(x_1/x_0)$], thus increasing the chances of external triggering. Although x_0 and v_i cannot be uniquely fixed, it is clear that, for reasonable values of these

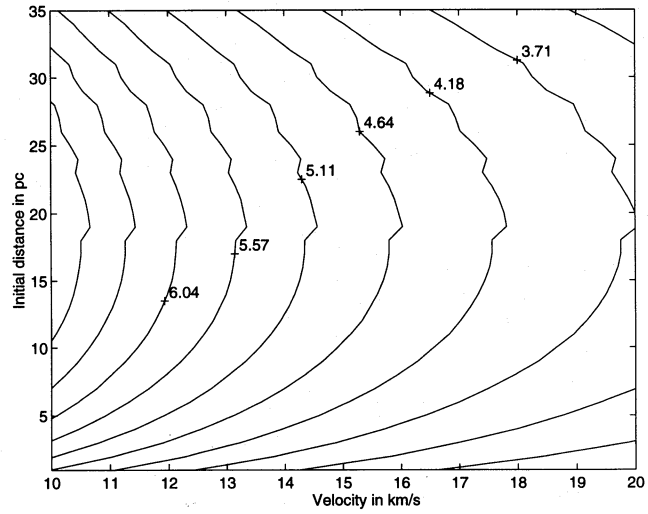

Figure 7. The contour plot of the time taken by the cloud L1616 to travel from its initial position to its present one, taken to be 50 pc, as a function of the initial distance, x_0, and the escape velocity of the ionized gas, v_i, when accelerated by the star ε Orionis through the rocket effect. Contours are labelled with the time taken in units of 10^6 years. The parameter space between the 4.2 and 5.1 Myr contours is favourable for the star being the external trigger.

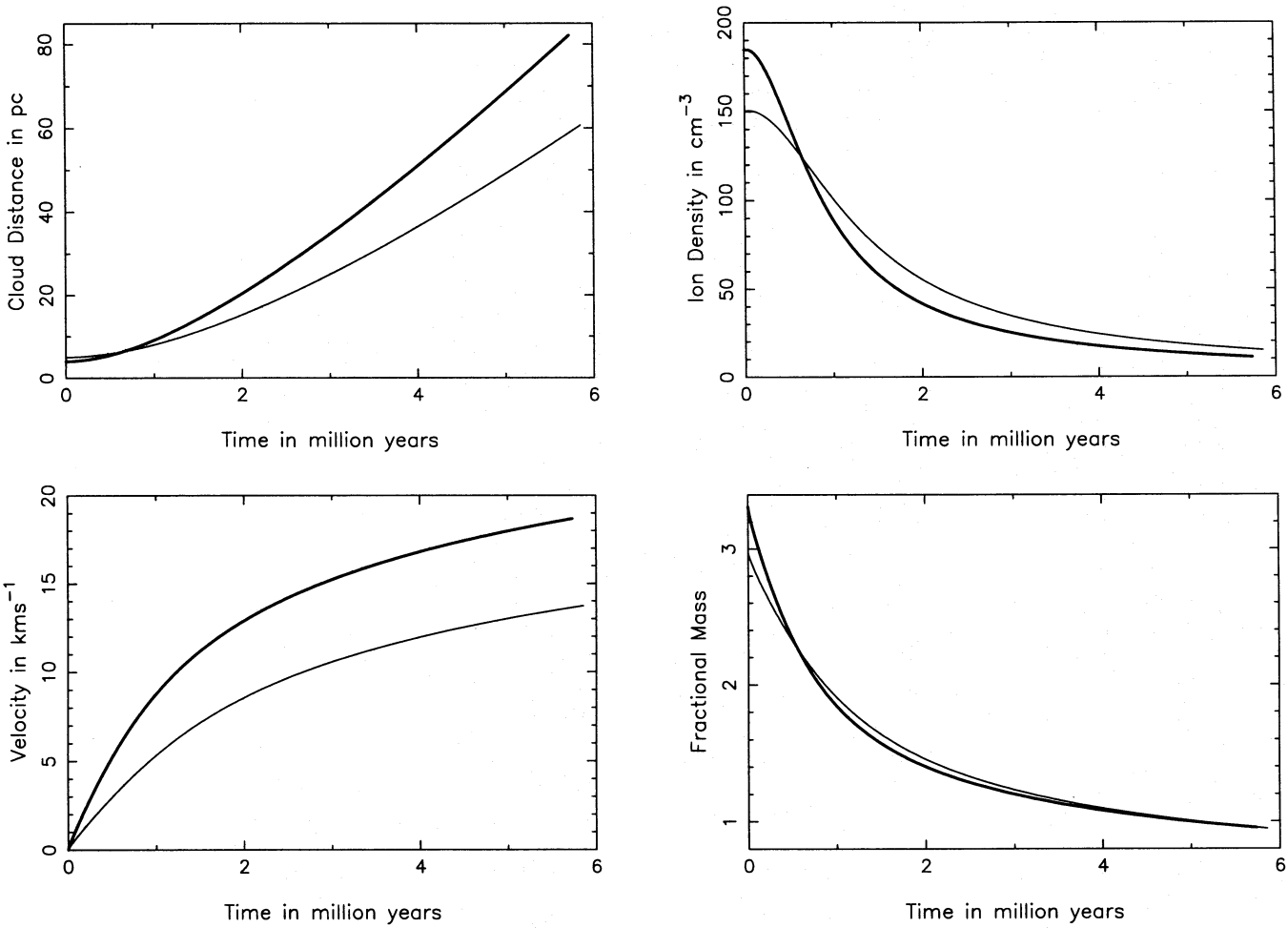

Figure 8. The time evolution of the cloud parameters as it is accelerated through the rocket effect. In each of the graphs, thin and thick curves correspond to two cases with v_i, x_0 and x_1 of 12 (15) km s^{-1}, 5 (4) pc and 50 (70) pc, respectively. Distance from the star, ion density just behind the shock front, velocity and mass expressed as a fraction of its present value, 180 $M_\odot$, are the respective parameters plotted in the four graphs.

© Royal Astronomical Society • Provided by the NASA Astrophysics Data System

1995MNRAS.276..923R

parameters, the progenitor of the star ε Orionis could have caused the propulsion of the cloud to its present position within the stellar lifetime. For a temperature of 10 000 K, the sound speed in the ionized plasma is ~ 11.4 km s^{-1} and, observationally, the plasma in a bright condensation in M16 is found to be streaming with a speed of ~ 13 km s^{-1} (Courtes, Cruvellier & Pottasch 1962). Hence, we take v_i to be typically between 12 and 15 km s^{-1}. The projected and 3D separation between the star and the cloud are 50 and 70 pc, respectively. If these are taken to be the lower and upper limits of the distance travelled in the maximum available time of ~ 5 Myr, along with a corresponding escape speed for the plasma of 12 and 15 km s^{-1}, the necessary initial separations turn out to be 5 and 4 pc, respectively. Fig. 8 shows the variation of the cloud parameters with time for these two cases. The corresponding initial mass, initial radius and the present speed of the cloud for the two cases are 535 $M_\odot$, 1.29 pc, 13.1 km s^{-1} and 595 $M_\odot$, 1.34 pc, 18.0 km s^{-1}, respectively. For the lower-velocity case, the measured radial velocity of ~ 7.5 km s^{-1}, which includes a galactic differential rotation contribution of ~ 3.7 km s^{-1}, would imply a proper-motion velocity of ~ 12.5 km s^{-1}. This would require that its direction of motion makes an angle $\gtrsim 73°$ with respect to the line of sight or, equivalently, the difference in the distance to the star and the cloud from the Sun is not more than ~ 15 pc. This is within the errors (~ 20 per cent) of the estimated distances to ε Orionis and L1616 of 370 pc and 420 pc, respectively. Incidentally, the density ρ_2 behind the shock front varies from 150 to 15 cm^{-3} (see Fig. 8). The density ahead of the front ρ_1 is approximately

$$\rho_1 = 2\rho_2 \left(\frac{v_2}{v_1}\right)^2$$

$$= 4\rho_2 \left(\frac{T_2}{T_1}\right), \qquad (4)$$

where the v's and T's are the corresponding sound speeds and temperatures. Taking T_1 and T_2 to be 40 and 10 000 K, respectively, ρ_1 is found to vary from 10^5 to 10^4 cm^{-3} over the last 5 Myr. This substantial density enhancement in the frontside of the cloud over a long period could have caused it to implode and form the cluster. The cloud fragmentation time-scale estimated earlier is consistent with this scenario. A quantity which could have substantiated this further is the tail-stretching time-scale. However, this could not be obtained, because there was no discernible velocity gradient along the tail. This may be a result of the insufficient velocity resolution used (0.65 km s^{-1} at 115 GHz). Also, it may be difficult to determine any possible gradient due to the confusion resulting from the mass motions in the cloud generated by the cluster. Nevertheless, assuming that the tail makes an angle of $\sim 73°$ with the line of sight, and the projected length of the tail is ~ 2.5 pc, the upper limit to the velocity gradient can be translated to a lower limit to the tail stretching time-scale of ~ 1.1 Myr. This agrees with the available travel time, but does not constrain it well. In conclusion, the above discussion is consistent with the hypothesis that the star ε Orionis has been the external trigger. A measurement of the proper-motion velocity of HD 293815, the brightest star exciting the reflection nebula, will confirm this.

5 SUMMARY

We shall now summarize our main findings. Our main objectives were to determine the mass of the cloud L1616 and to find out if large-scale mass motions are present. For this purpose, we mapped this cloud in the $J = 1 \rightarrow 0$ transitions of both ^{12}CO and ^{13}CO. We have presented the distributions of the ^{13}CO column density, the kinetic temperature, the equivalent width and the integrated line intensity in the cloud. They clearly indicate that the star cluster exciting the reflection nebula is the dominant energy source and that substantial mass motions are present in the cloud. The masses determined from the maps of ^{13}CO column density and ^{12}CO integrated line intensity are in agreement with each other, and suggest that the mass of the cloud L1616 is ~ 180 $M_\odot$. This confirms the high star formation efficiency suspected in this cloud if the stellar mass estimated from the FIR fluxes is reasonably correct. However, the virial mass estimated from the cloud-averaged linewidth of ~ 3 km s^{-1} is 1000 $M_\odot$. This is much larger than the above estimates and suggests that the cloud may be disintegrating. The evidence for mass motions supports this. The cometary appearance, the location of the star cluster near the edge facing the bright Orion stars, and the estimated high star formation efficiency suggest that the cluster formation may have been externally triggered. The star ε Orionis located opposite to the tail direction is the most likely external trigger. It is found that this star could have propelled the cloud from its initial distance to its present position in a time-scale of ~ 5 Myr for reasonable values of the two parameters, viz. the initial distance to the cloud from the star and the escape velocity of the ionized gas. If the cluster formation is externally triggered, the average density enhancement must have been high. This requires that the cloud be initially close to the star, which leads to a large space velocity of ~ 13 km s^{-1} at present. Then, the measured radial velocity requires the cloud to have a proper-motion velocity of ~ 12 km s^{-1}.

ACKNOWLEDGMENTS

I am grateful to the faculty of the Joint Astronomy Program, Department of Physics, Indian Institute of Science, Bangalore for providing me an opportunity to undertake research in astronomy. My sincere thanks are due to the staff of the Millimeterwave Laboratory and the Observatory at the Raman Research Institute for their help and support during the observations. I am also thankful to K. R. Anantharamiah and T. K. Sridharan for their critical comments on the manuscript, and to the anonymous referee for the useful suggestions and critical comments.

The study was carried out under the auspices of the Joint Astronomy Program, Department of Physics, Indian Institute of Science, Bangalore, in partial fulfilment of the requirements for the degree of Doctor of Philosophy.

REFERENCES

Allen C. W., 1976, Astrophysical Quantities. William Clowes and Sons, London, p. 209

Bally J., Langer W. D., Wilson R. W., Stark A. A., Pound M. W., 1991, in Falgarone E., Boulanger F., Duvert G., eds, Proc. IAU

© Royal Astronomical Society • Provided by the NASA Astrophysics Data System

1995MNRAS.276..923R

Symp. 147, Fragmentation of Molecular Clouds and Star Formation. Kluwer, Dordrecht, p. 11
Bertoldi F., 1989, ApJ, 346, 735
Bertoldi F., McKee C. F., 1990, ApJ, 354, 529
Courtes G., Cruvellier P., Pottasch S. R., 1962, Ann. d'Astroph., 25, 214
de Vries C. P., Brand J., Israel F. P., de Graauw Th., Wouterloot J. G. A., van de Sadt H., Habing H. J., 1984, A&AS, 56, 333
Dickman R. L., 1978, ApJS, 37, 407
Evans II N. J., Lada E. A., 1991, in Falgarone E., Boulanger F., Duvert G., eds, Proc. IAU Symp. 147, Fragmentation of Molecular Clouds and Star Formation. Kluwer, Dordrecht, p. 293
Feitzinger J. V., Stuwe J. A., 1984, A&AS, 58, 365
Hartley M., Manchester R. R., Smith R. M., Trittou S. B., Gross W. M., 1986, A&AS, 63, 27
Herbst W., 1975, AJ, 80, 212
Hirshfeld A., Sinnott R. W., 1985, Sky Catalogue 2000.0 Vol. 2. Cambridge Univ. Press, Cambridge
Indrani C., Sridharan T. K., 1994, JA&A, 15, 157
Lada C. J., 1991, in Lada C. J., Kylafis N. D., eds, NATO ASI series C, 342, The Physics of Star Formation and Early Stellar Evolution, Kluwer. Dordrecht, p. 329
Larson R. B., 1981, MNRAS, 194, 809
Lynds B. T., 1962, ApJS, 7, 1
Margulis M., Lada C. J., Young E. T., 1989, ApJ, 345, 906
Myers P. C., Fuller G. A., Mathieu R. D., Beichman C. A., Benson P. J., Schild R. E., Emerson J. P., 1987, ApJ, 319, 340
Oort J. H., Spitzer L., 1955, ApJ, 121, 6
Patel N. A., 1990, PhD thesis, Indian Institute of Science, Bangalore
Patel N. A., Xie T., Goldsmith P. F., 1993, ApJ, 413, 593
Racine R., 1968, AJ, 73, 223
Spitzer L., 1978, Physical Processes in the Interstellar Medium. John Wiley and Sons, New York, p. 262
Sridharan T. K., 1992, JA&A, 13, 217
Sridharan T. K., 1993, Bull. Astron. Soc. India, 21, 339
Strong A. W. et al., 1988, A&A, 207, 1
van den Bergh S., 1966, AJ, 71, 990
van den Bergh S., Herbst W., 1975, AJ, 80, 208
Witt A. N., Schild R. E., 1986, ApJS, 62, 839

APPENDIX A: EVOLUTION OF CLOUD PARAMETERS UNDER ROCKET ACCELERATION

An early-type star, when first formed, is expected to pump UV photons into the surrounding ISM rather abruptly. Many dense molecular condensations within its Stromgren radius (which is 12 pc for a star of spectral type O6V for an assumed value of 10 cm^{-3} for the mean hydrogen density of the surrounding medium) will experience a weak R-type ionization front passing quickly around them, after which the stellar UV radiation will drive an ionization front into the denser cloud. The ionized hydrogen produced on the side of the cloud facing the star, being at a higher pressure than the gas outside as a result of its higher density, would expand producing a recoil on the cloud, and thus accelerate it away from the star. The loss of this gas also results in the reduction of the cloud mass, and hence the cloud radius. In this appendix we derive equations describing how the cloud's position x, radius r, mass m and relative velocity with respect to the star v change with time under certain assumptions. Let v_1, m_1 and r_1, respectively, be the present velocity, mass and radius of the cloud and x_0 and x_1, respectively, be its initial and present distance from the star ε Orionis. Integrating the equation of motion, and taking v to be zero initially, one gets the following result for rocket acceleration:

$$M(v) = M_1 \exp\left(\frac{v_1 - v}{v_i}\right) = M_1 \exp(z_1 - z). \quad \text{(A1)}$$

Here, z is v expressed as a fraction of v_i, the velocity at which the ionized gas escapes. The latter is nearly equal to the sound speed in the ionized plasma which is ~ 11.4 km s^{-1}. In obtaining the above result we have ignored the deceleration due to sweeping up of matter. A cloud of radius ~ 1 pc ploughing through a median with an average hydrogen density of 1 cm^{-3} over a distance of ~ 70 pc would sweep up only a mass of $\sim 4\ M_\odot$. Since this is much smaller in comparison to the present cloud mass, deceleration arising from it can be ignored. This is particularly justified in the case of L1616 because the cloud is at an altitude of ~ -190 pc while the star ε Orionis is at an altitude of ~ -120 pc (their galactic longitudes and latitudes are (203.5, −24.7) and (205.2, −17.2), respectively). Thus, most of the motion of L1616 would have taken place at high altitudes, nearly perpendicular to the galactic plane, where the general ISM density is likely to be quite low resulting in negligible swept-up mass.

The rate at which the cloud loses mass is given by $m_p n(z) \pi r^2(z) v_i$, where m_p is the mass of a proton and $n(z)$ is the number density of hydrogen ions just behind the ionization front (Spitzer 1978). Here, both n and r are taken to depend on z. As the cloud recedes from the star, the ionizing photon density at the cloud surface will vary and hence cause n to vary. Since the cloud loses mass, the cloud radius would also change. If the mean density is conserved, then $r(z)$ is given by,

$$r(z) = r_1 \exp\left(\frac{z_1 - z}{3}\right). \quad \text{(A2)}$$

Assuming that the gas expands spherically and that the recombinations occurring in it almost completely *shield* the stellar UV photons, one obtains the following expression for $n(z)$ (Spitzer 1978):

$$n(z) = \frac{1}{x(z)} \sqrt{\frac{3N_c}{4\pi\alpha r(x)}}, \quad \text{(A3)}$$

where N_c is the stellar output rate of ionizing photons and α is the effective recombination probability for hydrogen taken to be 2.6×10^{-13} cm^3 s^{-1}. Now, equating the mass-loss rate to $M(z)/v_i\ (dv/dt)$ and solving for $x(z)$ using the fact that $dz/dt = v_i z (dz/dx)$, one obtains

$$x(z) = x_0 \exp\left\{\beta\left[\exp(0.5z_1) - (1 + 0.5z)\exp\left(\frac{z_1 - z}{2}\right)\right]\right\} \quad \text{(A4)}$$

where

$$\beta = \frac{4M_1}{m_p}\sqrt{\frac{4\alpha}{3\pi N_c r_1^2}}. \quad \text{(A5)}$$

© Royal Astronomical Society • Provided by the NASA Astrophysics Data System

1995MNRAS.276..923R

It is worth noting that, in addition to their boundary values, the cloud variables described by the above equations depend only on z and not on v or v_i themselves. The fact that the infinitesimal time dt taken for the cloud to move by an infinitesimal distance dx depends on the velocity and acceleration during that period results in the following equation:

$$dt(z) = \frac{\beta x(z) \exp[(z_1 - z)/2]}{8v_i} \times \left\{ -z + \sqrt{z^2 + \frac{16 \exp[(z - z_1)/2]\, dx}{\beta x(z)}} \right\}. \quad \text{(A6)}$$

Since it was not possible to obtain a closed form solution, we have numerically integrated this equation to get the time as a function of z. In the graphs shown in Fig. 8, the time axis was derived in this way.

© Royal Astronomical Society • Provided by the NASA Astrophysics Data System